

CLAIRAUT'S EQUATION EXTENDED TO FAST ROTATORS

C. Staelen¹ and J.-M. Huré¹

Abstract. In the theory of Nested Spheroidal Figures of Equilibrium (NSFoE, see Huré 2022), rotating bodies are decomposed into thick, homogeneous layers bounded by spheroids. The associated set of equations, which uses Maclaurin's formula for the homogeneous spheroid, admit accurate solutions, provided the interfaces between layers are very close to confocal (in the sense of spheroidal oblate coordinates). In this contribution, we present a few results obtained in the continuous limit, i.e. when the number of spheroidal layers is infinite, thereby enabling to model full heterogeneity. In particular, we derive an integro-differential equation which basically contains Clairaut's fundamental equation, but which works also for fast rotators (Staelen & Huré 2023). The solutions compare very well to numerical solutions obtained from the Self-Consistent-Field method. A few examples are given.

Keywords: Gravitation, stars: interiors, planets and satellites: interiors, Methods: analytical

1 Introduction

Two hundred and eighty years ago, Clairaut (1743) published a major theory for the figure of the Earth as a heterogeneous fluid mass in slight deviation from sphericity. He showed that, in the limit of small flattenings, the isopycnic surfaces are very close to spheroids (i.e. ellipsoids of revolution). Clairaut was able to derive a powerful second-order differential equation for the eccentricity ε as a function of the equatorial radius a , namely

$$\frac{d^2\varepsilon^2}{da^2} + \frac{2}{a} \frac{a^3\rho(a)}{\int_0^a da'\rho(a')a'^2} \frac{d\varepsilon^2}{da} + \frac{2}{a^2} \left[\frac{a^3\rho(a)}{\int_0^a da'\rho(a')a'^2} - 3 \right] \varepsilon^2(a) = 0, \quad (1.1)$$

where ρ the mass density along the given isopycnic. So, provided the mass-density profile is known in advance (which is generally not the case), the eccentricity can be determined with appropriate boundary conditions (BCs). We have typically $d\varepsilon^2/da = 0$ at the center and a value ε_s can be prescribed at the surface. The internal structure is then fully solved. Clairaut's equation is valid only for small values of ε^2 , i.e. for slow rotators. If this is justified for the Earth ($\varepsilon_s^2 \sim 7 \times 10^{-3}$) and for the Sun ($\varepsilon_s^2 \sim 2 \times 10^{-5}$), objects like Ceres ($\varepsilon_s^2 \sim 1 \times 10^{-1}$), Saturn ($\varepsilon_s^2 \sim 2 \times 10^{-1}$) and Achernar ($\varepsilon_s^2 \sim 4 \times 10^{-1}$) are clearly not accessible by Clairaut's theory. Lanzano (1974) has considered faster rotators by expanding both the shape and the gravitational potential on Legendre polynomials P_{2m} for any order m ; thus the ellipsoidal shape is forsaken for a more general one. This method has been used at second-order for the Earth by Chambat et al. (2010), and at third-order for Ceres by Rambaux et al. (2015). In this work, however, we keep the spheroidal shape for all isopycnic surfaces and we study the quality of this approximation for fast rotators.

2 An integro-differential equation for the general problem

As early formulated by Poincaré and prolonged by Hamy (1890), a spheroidal stratification can not represent an exact physical equilibrium for any rotation rate, mainly because this would require both a confocal stratification of layers and a density inversion from centre to surface. This is Hamy's "no-go" theorem. Both classical theories and modern models predict a fully reversed situation: for real systems isopycnic surfaces are more spherical at the centre than close to the surface and the mass-density gradient is essentially negative. We

¹ Univ. Bordeaux, CNRS, LAB, UMR 5804, F-33600 Pessac, France

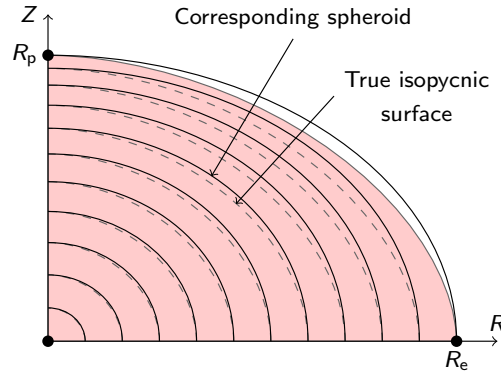


Fig. 1. Schematic diagram of the spheroidal approximation made in this work.

have build a \mathcal{L} -layer theory by superposing homogeneous spheroids with different mass densities and ellipse parameters (Hur e 2022). Actually, in this kind of problem, the calculation of the gravitational potential is a major difficulty, and considering such structures is particularly attractive as the potential is exceptionnally known in closed-form. This is also widely supported by the numerical experiments which show that isopycnic surfaces are very close to spheroids (Kong et al. 2015; Basillais & Hur e 2021). In the limit $\mathcal{L} \rightarrow \infty$, the body becomes continuously inhomogeneous, instead of piece-wise inhomogeneous. By converting discrete summations and differences to integrals and derivatives, we can derive a new equation relating the mass density and the eccentricity profile. This is an integro-differential equation (IDE) of the form

$$\frac{d\varepsilon^2}{da} = \frac{2 \int_{\rho(0)}^{\rho(a)} d\rho(a') \chi(a', a; \varepsilon)}{\int_{\rho(0)}^{\rho(1)} d\rho(a') \mu(a', a; \varepsilon)}, \quad (2.1)$$

which tends to Clairaut's equation for $\varepsilon^2 \ll 1$. The two functions χ and μ (not reported here; see Staelen & Hur e 2023) are continuous and smooth on the whole domain of interest, i.e. for $a \in [0, R_e]$, where R_e is the equatorial radius.

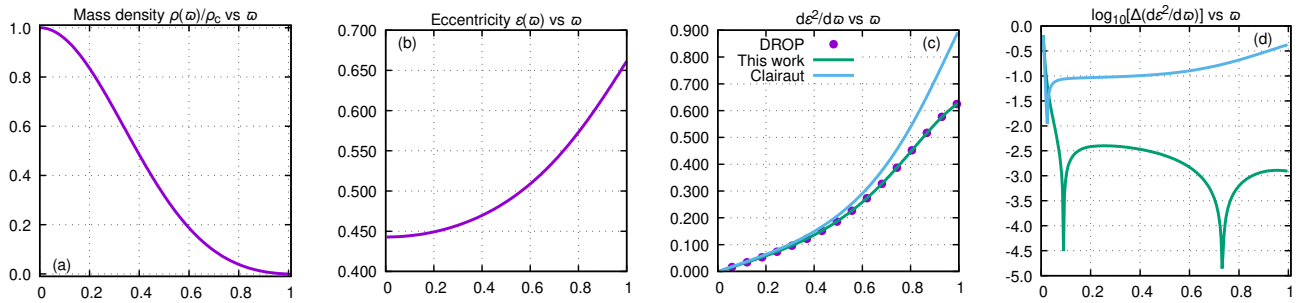


Fig. 2. The mass density obtained with the DROP-code (see in the text) in the equatorial plane (panel a) and the eccentricity profile (panel b) versus the normalised radius $\varpi = a/R_e$ obtained for a polytrope with axis ratio 0.75 and index $n = 1.5$. The self-consistency check of the IDE (panel c) compares both side of (2.1) computed from these reference profiles. Also shown is the derivative computed from Clairaut's equation, and the absolute deviations (panel d).

3 Validation of the IDE by a numerical reference

Regardless of any physical solution of (2.1) that could be produced for a given objects, it is possible to check its precision simply by comparing the LHS and th RHS when fed by a numeral solution. In this purpose, we use the multilayer version of the DROP code (Basillais & Hur e 2021), which solves the equilibrium of self-gravitating fluid a from the self-consistent field method. Without loss of generality, we work under axisymmetry and use a

polytropic fluid*. Once a solution is obtained, we first extract the mass-density along the equatorial plane $\rho(a)$, and compute a pseudo-eccentricity $\sqrt{1 - b^2/a^2}$ defined as the eccentricity of the isopycnic surfaces (which are not perfect spheroids) that hits the polar axis at $Z = b$ and the equatorial axis at $R = a$. We then inject these profiles into the integrals in the RHS of the IDE, and we then get $(d\varepsilon^2/da)^{1D}$. Second, we compute directly the derivative of the pseudo-eccentricity still output by the 2D-code, and we get directly $(d\varepsilon^2/da)^{2D}$. These two derivatives can then be compared. As an illustration, we give in Fig. 2 the results obtained in the case where the ratio between the polar radius and the equatorial radius is 0.75 (a fast rotator) and where the polytropic index is $n = 1.5$ (this value corresponds for instance to a fully convective star). We see that the discrepancy between the IDE and the DROP-code is below 3×10^{-3} , typically (against 3×10^{-1} for Clairaut), which is very good. The IDE thus allows to access easily fast rotators, as the error is still low for highly flattened objects.

4 The case of mass-density jumps. An application to the Earth

We have tested the behaviour of the IDE in the case of the Earth, by using the Preliminary Reference Earth Model (PREM, Dziewonski & Anderson 1981). This is a seismologic model assuming a *spherical* (i.e. non-rotating) planet. As a matter of fact, (2.1) is able to account for mass-density jumps (the PREM presents several discontinuities; see Fig 3a), but this requires an additional technical effort. We first write the mass density as

$$\rho(\varpi) = \sum_{k=1}^{\mathcal{K}} [\rho_k(\varpi) - \rho_{k+1}(\varpi)] \mathcal{H}(\varpi_k - \varpi), \quad (4.1)$$

with ρ_k as the mass density inside domain k , ϖ_k as the position of the mass density jump between domains k and $k + 1$ and \mathcal{H} as Heaviside's distribution. Remembering that the derivative (in the sense of distributions) of $\mathcal{H}(x)$ is Dirac's distribution $\delta(x)$, we obtain for any continuous function f on $[0, 1]^2$

$$\int_{\rho(0)}^{\rho(1)} d\rho(\varpi') f(\varpi', \varpi) = \sum_{k=1}^{\mathcal{K}} \int_{\rho(\varpi_{k-1})}^{\rho(\varpi_k)} d\rho_k(\varpi') f(\varpi', \varpi) - \sum_{k=1}^{\mathcal{K}} \frac{\alpha_k - 1}{\alpha_k} \rho_k(\varpi_k) f(\varpi_k, \varpi) \quad (4.2)$$

where $\alpha_k = \rho_k(\varpi_k)/\rho_{k+1}(\varpi_k)$ is the mass density jump at the interface between domains k and $k + 1$, which occurs at ϖ_k . Thus, (4.2) can be used to compute the RHS of (2.1). Then, we have written an algorithm to solve iteratively (2.1) with the mass density profile given by Dziewonski & Anderson (1981) as an input. We first initialise the eccentricity profile with a generic parabola (from center to surface), then compute $d\varepsilon^2/da$ from (2.1), and deduce a new eccentricity profile by integration. This is repeated until the ε -profile converges. As BCs, we impose $1 - \sqrt{1 - \varepsilon_s^2} = 1/298.257\dots$ as the flattening. To make the numerical treatment easier, the mass density is normalised by its central value ρ_c , i.e. $\rho_c = 13088.5 \text{ kg} \cdot \text{m}^{-3}$.

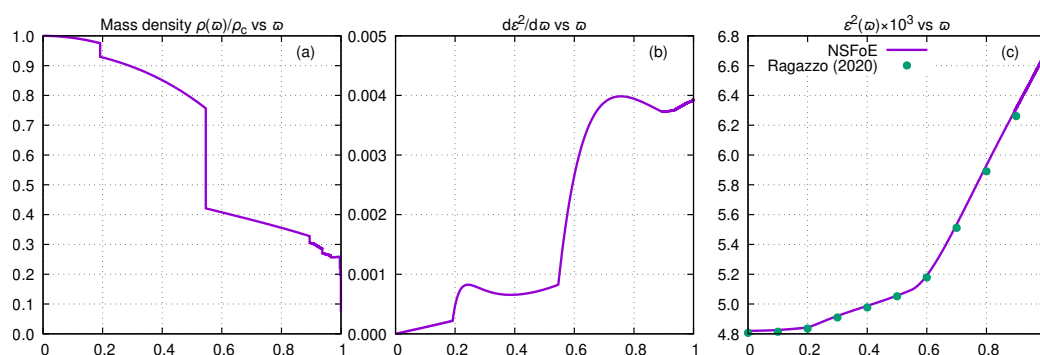


Fig. 3. Numerical solution for the eccentricity profile (panels b and c) versus the normalised radius inside the Earth using the “normalised PREM” as an input (panel a). Data computed by Ragazzo (2020) is also plotted.

The results are plotted in figure 3. We show in panel (a) the mass-density (the main input), and in panels (b) and (c) $d\varepsilon^2/da$ and ε^2 respectively. We have also reported the results obtained by Ragazzo (2020) scanned,

*The pressure P is related to the mass density ρ by $P = K\rho^{1+1/n}$, where K and n are positive constants.

Quantity (unit)	(Chambat et al. 2010)	This work
Mass (kg)	5.97218×10^{24}	
Equatorial radius (m)	6.378137×10^6	
Normalised MOI (-)	3.3069×10^{-1}	3.3151×10^{-1}
Rotation rate (s^{-1})	7.2921×10^{-5}	7.3104×10^{-5}
2nd degree gravitational moment (-)	1.0826×10^{-3}	1.0771×10^{-3}
4th degree gravitational moment (-)	-1.620×10^{-6}	-2.8233×10^{-6}
Relative Virial parameter		6×10^{-7}

Table 1. Physical properties of the Earth rescaled on the observed mass and equatorial radius and comparison with the data from Chambat et al. (2010).

who has solved Clairaut’s equation, i.e. (1.1), with the same mass density prescription. We see that both solutions are in excellent agreement, with a slight deviation at large radii (i.e. close to the outermost surface).

The main output data are listed on Tab. 1, where we have also listed the values given by Chambat et al. (2010). Our dimensionless results have been rescaled with the mass and the radius given therein. The agreement with our approach is good, within a few 10^{-3} . The discrepancies have a priori two origins: the mass-density profile, which, in our case, comes from the *non-rotating* PREM (i.e. $\varepsilon^2 = 0$, while we find $\varepsilon^2 \sim 5 \times 10^{-3}$), and the slight deviation to spheroids assumed in Chambat et al. (2010). As the Virial parameter[†] of our solution is about 10^{-6} , this means the spheroidal approximation is very good; thus the use of a non-rotating model for a rotating planet seems to be the main source of error.

5 Conclusions

We have derived an integro-differential equation (IDE) describing the equilibrium of a spheroidally stratified body in the framework of the NSFoE theory, which is based on Maclaurin’s formula. Although such equilibria remain approximate (see Hamy’s “no-go” theorem), we have shown that this IDE was a reliable approximation even for fast rotators, with errors about 10^{-3} in relative. We then have built a code solving numerically the IDE in the case of a prescribed mass-density profile, which may contain several discontinuities. We have then computed the eccentricity profile for a rotating Earth, with the mass density obtained by seismologic models for a non-rotating Earth as an input. Our results were in accordance with Chambat et al. (2010), with an accuracy of much less than a percent.

We would like to thank J. Lambert, N. Rambaux and S. Rosat for fruitful comments and discussions during the session.

References

- Basillais, B. & Huré, J.-M. 2021, MNRAS, 506, 3773
Chambat, F., Ricard, Y., & Valette, B. 2010, Geophysical Journal International, 183, 727
Clairaut, A. C. 1743, Théorie de la figure de la Terre tirée des principes de l’hydrostatique (David Fils)
Dziewonski, A. M. & Anderson, D. L. 1981, Physics of the Earth and Planetary Interiors, 25, 297
Hamy, M. 1890, Journal de mathématiques pures et appliquées. Tome VI, Gauthier-Villars et Fils, 69
Huré, J.-M. 2022, MNRAS, 512, 4047
Kong, D., Zhang, K., & Schubert, G. 2015, Physics of the Earth and Planetary Interiors, 249, 43
Lanzano, P. 1974, Ap&SS, 29, 161
Ragazzo, C. 2020, São Paulo Journal of Mathematical Sciences, 14, 1
Rambaux, N., Chambat, F., & Castillo-Rogez, J. C. 2015, A&A, 584, A127
Staelen, C. & Huré, J.-M. 2023, MNRAS, under revision

[†]The relative Virial parameter RVP is defined as $RVP = (W + 2T + U)/|W|$, where W , T and U are the gravitational, kinetic and internal energies, respectively. The lower $|RVP|$, the closer the solution is to exact equilibrium.